Biochemical Pharmacology 180 (2020) 114144

Contents lists available at ScienceDirect

Biochemical Pharmacology

journal homepage: www.elsevier.com/locate/biochempharm

Design and pharmacological profile of a novel covalent partial agonist for the adenosine A_1 receptor

Xue Yang[1], Majlen A. Dilweg[1], Dion Osemwengie, Lindsey Burggraaff, Daan van der Es, Laura H. Heitman, Adriaan P. IJzerman*

Division of Drug Discovery and Safety, Leiden Academic Centre for Drug Research (LACDR), Leiden University, P.O. Box 9502, 2300RA Leiden, The Netherlands

ARTICLE INFO

Keywords:
G protein-coupled receptors
Adenosine A_1 receptor
Covalent ligand
Partial agonist
Radioligand binding
Label-free assay

ABSTRACT

Partial agonists for G protein-coupled receptors (GPCRs) provide opportunities for novel pharmacotherapies with enhanced on-target safety compared to full agonists. For the human adenosine A_1 receptor (hA_1AR) this has led to the discovery of capadenoson, which has been in phase IIa clinical trials for heart failure. Accordingly, the design and profiling of novel hA_1AR partial agonists has become an important research focus. In this study, we report on LUF7746, a capadenoson derivative bearing an electrophilic fluorosulfonyl moiety, as an irreversibly binding hA_1AR modulator. Meanwhile, a nonreactive ligand bearing a methylsulfonyl moiety, LUF7747, was designed as a control probe in our study.

In a radioligand binding assay, LUF7746's apparent affinity increased to nanomolar range with longer pre-incubation time, suggesting an increasing level of covalent binding over time. Moreover, compared to the reference full agonist CPA, LUF7746 was a partial agonist in a hA_1AR-mediated G protein activation assay and resistant to blockade with an antagonist/inverse agonist. An *in silico* structure-based docking study combined with site-directed mutagenesis of the hA_1AR demonstrated that amino acid $Y271^{7.36}$ was the primary anchor point for the covalent interaction. Additionally, a label-free whole-cell assay was set up to identify LUF7746's irreversible activation of an A_1 receptor-mediated cell morphological response.

These results led us to conclude that LUF7746 is a novel covalent hA_1AR partial agonist and a valuable chemical probe for further mapping the receptor activation process. It may also serve as a prototype for a therapeutic approach in which a covalent partial agonist may cause less on-target side effects, conferring enhanced safety compared to a full agonist.

1. Introduction

G protein-coupled receptors (GPCRs) are one of the largest families of drug targets [1]. Being transmembrane proteins they, however, pose problems in studying their structure and function, due to their low expression and profound instability. To solve these problems, covalent ligands have been shown to be useful tools for the structure elucidation of active/inactive receptor structures and mapping of the ligand-binding domains [2]. Beyond that, covalent ligands are beginning to be applied in GPCR chemical biology and proteomics applications [3].

Historically, the few covalent agonists for the human adenosine A_1 receptor (hA_1AR) available have all been derivatives of the endogenous ligand adenosine, containing an intact ribose moiety. Chemical modification of the adenosine structure at the N^6 position has yielded several selective chemoreactive agonists [4,5]. One such example is N^6-[4-[[[4-[[[[2-[[[(m-isothiocyanatophenyl)amino]-thiocarbonyl]amino]ethyl]amino]carbonyl]methyl]aniline]-carbonyl]methyl]phenyl]adenosine (m-DITC-ADAC), an adenosine analogue incorporating a chemoreactive isothiocyanate group to form a covalent bond with the receptor [5]. These covalent agonists were validated as full agonists for the adenosine A_1 receptor [6,7]. However, full activation of the hA_1AR influences a broad physiologic spectrum of cardiac functions associated with unwanted effects, such as atrioventricular block [7]. Thus, partial agonists, triggering submaximal effects compared to a full agonist, have emerged as a new therapeutic option in treating cardiovascular indications [8]. Research from Bayer and our group has unveiled the existence of 2-aminopyridine-3,5-dicarbonitrile derivatives such as capadenoson and LUF5853 as non-ribose agonists for the hA_1AR (Fig. 1) [9–11]. Here, we used the 2-aminopyridine-3,5-dicarbonitrile scaffold as a starting point in our design and synthesis efforts towards a covalent

* Corresponding author.
E-mail address: ijzerman@lacdr.leidenuniv.nl (A.P. IJzerman).
[1] These authors contributed equally to this work.

https://doi.org/10.1016/j.bcp.2020.114144
Received 31 March 2020; Received in revised form 3 July 2020; Accepted 7 July 2020
Available online 10 July 2020

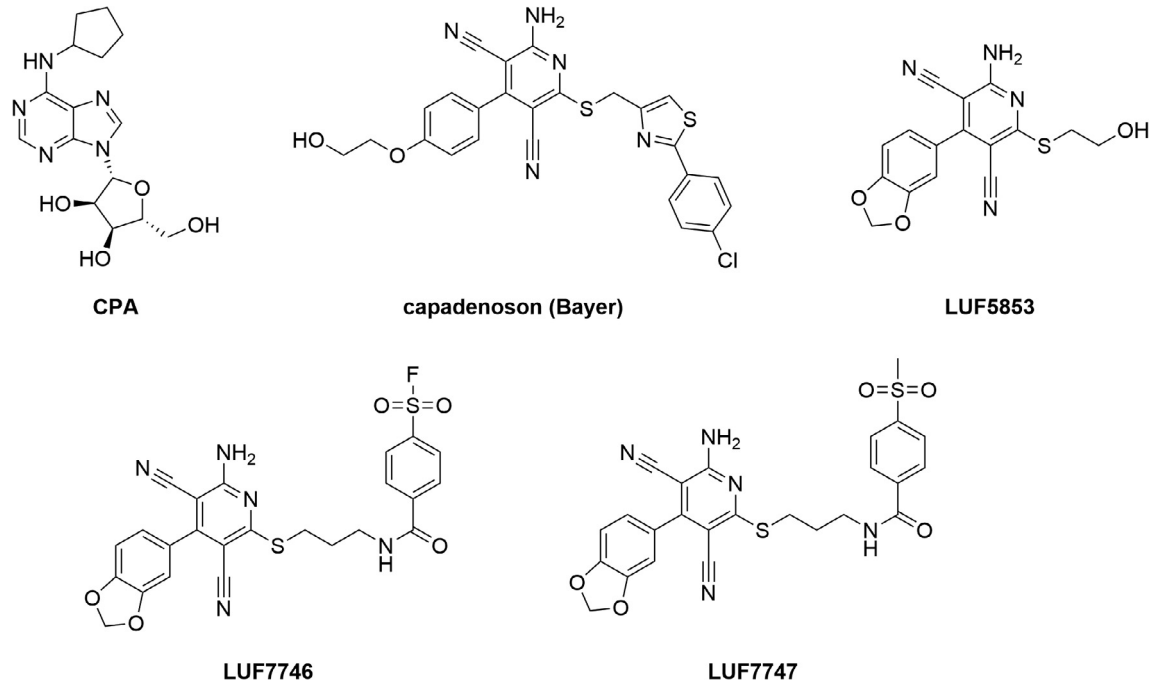

Fig. 1. Chemical structures of reference (non-ribose) hA_1AR agonists (top) and non-ribose hA_1AR agonists from this study (bottom).

partial agonist probe for the hA_1AR, the fluorosulfonyl-equipped derivative LUF7746. Moreover, a chemically similar, but non-reactive methylsulfonyl-equipped ligand, LUF7747, was designed to be used as a reversible control ligand. We then validated LUF7746 to bind covalently and partially activate the receptor in a series of *in vitro* experiments. We finally provided evidence for its point of attachment to the receptor. The results presented here constitute the initial report and pharmacological profiling of a novel, non-ribose covalent partial agonist and also shed light on the rational design of partial agonists as therapeutics. Furthermore, this reported covalent ligand could serve as a valuable pharmacological tool to investigate the contribution of partial activation of hA_1AR physiological functions.

2. Materials and methods

2.1. Chemistry (Scheme 1)

All solvents and reagents were purchased from commercial sources and were of analytical grade. Demineralised water is referred to as H_2O, as was used in all cases unless stated otherwise (i.e., brine). All reactions were routinely monitored with thin layer chromatography (TLC), using aluminium silica gel coated 60 F_{254} plates from Merck. Purification by column chromatography was carried out with the use of VWR silica gel irregular ZEOprep® particles (60–200 μm). Solutions were concentrated using a Heidolph Hei-VAP Value rotary evaporator. Nuclear magnetic resonance (NMR) spectra were recorded on a Bruker AV-400 liquid spectrometer (^{1}H NMR, 400 MHz) at ambient temperature and subsequently analysed with MestReNova v.12 software. Chemical shifts are reported in parts per million (ppm), designated by δ and corrected to the internal standard tetramethylsilane (δ = 0). Coupling constants are reported in Hz and are designated as *J*. Mass analyses were performed with liquid chromatography mass spectrometry (LC-MS) using an LCQ™ Advantage MAX system from Thermo Finnigan together with a Phenomenex Gemini® C18 110 Å column (50 mm × 4.6 mm × 3 μm). Samples were eluted using an isocratic system of H_2O/CH_3CN/1% TFA in H_2O, through decreasing the polarity of the solvent mixture from 80:10:10 to 0:90:10 in an elution time of 15 min. Analytical purity of the obtained final compounds was determined with high performance liquid chromatography (HPLC) using a Shimadzu HPLC system with a Phenomenex Gemini® C18 110 Å column (50 mm × 4.6 mm × 3 μm) coupled to a 254 nm UV detector. Samples were eluted using the same method as mentioned for LC-MS. For both LC-MS and HPLC, 0.3–0.8 mg of compound was dissolved in 1 mL of a 1:1:1 mixture of CH_3CN/H_2O/tBuOH as sample preparation. All reactions were performed under nitrogen atmosphere unless stated otherwise. Ligands were synthesized in a two step protocol as described below from the previously reported compound **1** (Scheme 1) [9,12].

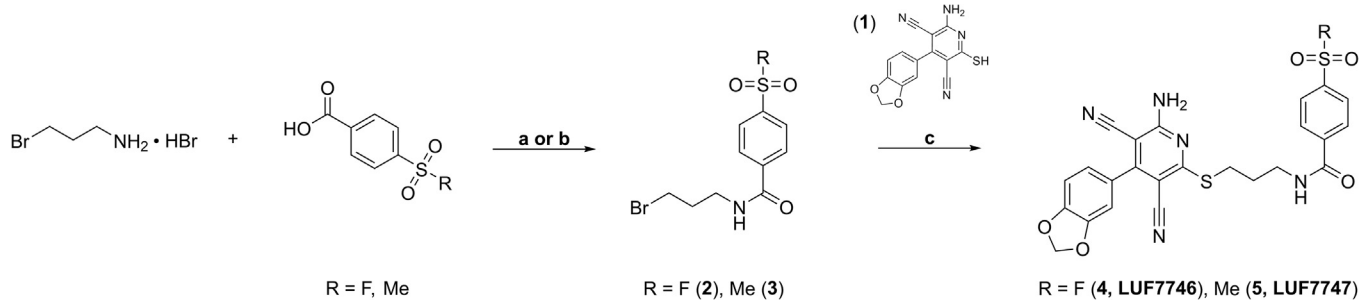

Scheme 1. Synthetic route towards partial hA_1AR agonists. Reagents and conditions: (a) EDC·HCl, DIPEA, DMF, 0 °C, 74%; (b) EDC·HCl, DMAP, DMF, rt, 26%; (c) $NaHCO_3$, DMF, rt, 8–45%.

2.1.1. 4-((3-((6-amino-4-(benzo[d][1,3]dioxol-5-yl)-3,5-dicyanopyridin-2-yl)thio)propyl)carbamoyl)benzenesulfonylfluoride (4, LUF7746)

A mixture of 4-(fluorosulfonyl)benzoic acid (1.5 mmol, 0.30 g, 1.0 equiv), 3-bromopropylamine hydrobromide (1.9 mmol, 0.42 g, 1.3 equiv) and EDC·HCl (1.8 mmol, 0.33 g, 1.2 equiv) in anhydrous DMF was cooled down to 0 °C. Subsequently, DIPEA (3.0 mmol, 0.52 mL, 2.0 equiv) was added dropwise and the solution was stirred for 4 h at 0 °C, followed by overnight stirring at room temperature. After completion was observed on TLC, the mixture was concentrated *in vacuo*. Water was added to the residue and the mixture was extracted three times with ethyl acetate. The combined organic layers were washed three times with 1 M HCl, dried over $MgSO_4$, filtered and concentrated *in vacuo*. The crude product was purified by column chromatography (EtOAc:PE = 1:2) to give the *N*-(3-bromopropyl)-4-(fluorosulfonyl) benzamide (**2**) as a white solid (1.1 mmol, 0.35 g, 74%). 2-amino-4-(benzo[*d*][1,3]dioxol-5-yl)-6-mercaptopyridine-3,5-dicarbonitrile **1** (0.48 mmol, 0.14 g, 1.0 equiv) was dissolved in anhydrous DMF in the presence of **2** (0.48 mmol, 0.15 g, 1.0 equiv) and $NaHCO_3$ (0.73 mmol, 0.061 g, 1.5 equiv) and stirred at room temperature until completion of the reaction. Water was added to the mixture which was extracted with EtOAc four times. Subsequently, the combined organic layers were washed with brine 4 times, dried over $MgSO_4$, filtered and concentrated *in vacuo*. The crude product was purified via column chromatography (EtOAc:PE = 50–100%) to yield the desired compound as white solid (0.039 mmol, 0.021 g, 8%). ^{1}H NMR (400 MHz, $CDCl_3$) δ 8.10 (d, J = 8.4 Hz, 2H), 8.02 (d, J = 8.3 Hz, 2H), 7.00 (dd, J = 8.0, 1.6 Hz, 1H), 6.97–6.92 (m, 2H), 6.55 (t, J = 5.6 Hz, 1H), 6.07 (s, 2H), 5.92 (br s, 2H), 3.65 (q, J = 6.7 Hz, 2H), 3.27 (t, J = 7.1 Hz, 2H), 2.16 (quin, J = 7.1 Hz, 2H) ppm. ^{13}C NMR (126 MHz, CDCl3) δ 168.6, 165.9, 159.8, 157.9, 150.0, 148.2, 140.9, 135.4, 128.8, 128.4, 126.8, 123.3, 115.6, 115,4, 108.9, 108.8, 102.0, 95.9, 86.5, 39.7, 39.5, 29.1, 28.0 ppm. MS: $[ESI + H]^+$: 540.0. HPLC t_R = 8.36 min, purity 97%.

2.1.2. N-(3-((6-amino-4-(benzo[d][1,3]dioxol-5-yl)-3,5-dicyanopyridin-2-yl)thio)propyl)-4-(methylsulfonyl)benzamide (5, LUF7747)

A mixture of (4-methylsulfonyl)-benzoic acid (0.82 mmol, 0.16 g, 1.0 equiv), 3-bromopropylamine hydrobromide (1.1 mmol, 0.23 g, 1.3 equiv) and EDC·HCl (0.98 mmol, 0.19 g, 1.2 equiv) in anhydrous DMF was stirred for 1 h at rt. Subsequently, DIPEA (1.7 mmol, 0.29 mL, 2.0 equiv) was added dropwise to the suspension and the reaction was stirred overnight at room temperature. After completion was observed on TLC, the mixture was concentrated *in vacuo*. Water was added to the residue and the mixture was extracted three times with ethyl acetate. The combined organic layers were washed three times with 1 M HCl, dried over $MgSO_4$, filtered and concentrated *in vacuo*. The crude product was purified by column chromatography (EtOAc:PE = 2:1) to give *N*-(3-bromopropyl)-4-(methylsulfonyl)benzamide **(3)** as a white solid (0.21 mmol, 0.068 g, 26%). 2-amino-4-(benzo[*d*][1,3]dioxol-5-yl)-6-mercaptopyridine-3,5-dicarbonitrile **1** (0.21 mmol, 0.062 g, 1.0 equiv) was dissolved in anhydrous DMF in the presence of **3** (0.21 mmol, 0.067 g, 1.0 equiv) and $NaHCO_3$ (0.31 mmol, 0.026 g, 1.5 equiv) and stirred at room temperature until completion of the reaction. Water was added to the mixture which was extracted with EtOAc four times. Subsequently, the combined organic layers were washed with brine 4 times, dried over $MgSO_4$, filtered and concentrated *in vacuo*. The crude product was purified via column chromatography (EtOAc:PE = 50–100%) to yield the desired compound as off-white solid (0.093 mmol, 0.050 g, 45%). ^{1}H NMR (400 MHz, DMSO-d_6) δ 8.80 (t, J = 5.6 Hz, 1H), 8.07 (d, J = 8.4 Hz, 2H), 8.02 (d, J = 8.4 Hz, 2H) 7.15 (d, J = 1.8 Hz, 1H), 7.10 (d, J = 8.1 Hz, 1H), 7.02 (dd, J = 8.1, 1.8 Hz, 1H), 6.15 (s, 2H), 3.43 (q, J = 6.6 Hz, 2H), 3.31–3.24 (m, 5H), 1.96 (quin, J = 7.0 Hz, 2H) ppm. ^{13}C NMR (126 MHz, DMSO-d_6) δ 167.5, 165.7, 160.2, 158.4, 149.5, 147.9, 143.4, 139.5, 128.7, 127.9, 127.6, 123.5, 116.1, 115.9, 109.5, 109.1, 102.4, 94.3, 86.4, 43.8, 38.9, 29.2, 27.9 ppm. MS: $[ESI + H]^+$: 535.9 HPLC t_R = 7.41 min, purity 99%.

2.2. Biology

Both radioligands 1,3-[^{3}H]-dipropyl-8-cyclopentylxanthine ([^{3}H] DPCPX, specific activity of 120 Ci × $mmol^{-1}$) and [2-^{3}H]-4-(2-[7-amino-2-(2-furyl)-[1,2,4]-triazolo-[2,3-*a*]-[1,3,5]-triazin-5-ylamino] ethyl ([^{3}H]ZM241385, specific activity of 50 Ci × $mmol^{-1}$) were purchased from ARC Inc. (St. Louis, MO). [^{3}H]PSB603 ([^{3}H]-8-(4-(4-(4-chlorophenyl)piperazide-1-sulfonyl)phenyl)-1-propylxanthine, specific activity 79 Ci × $mmol^{-1}$) and [^{3}H]-8-Ethyl-4-methyl-2-phenyl-(8*R*)-4,5,7,8-tetrahydro-1*H*-imidazo[2,1-*i*]-purin-5-one ([^{3}H]PSB-11, specific activity 56 Ci × $mmol^{-1}$) were obtained with kind help of Prof. C.E. Müller (University of Bonn, Germany). [^{35}S]-guanosine 5'-(γ-thio)triphosphate ([^{35}S]GTPγS, specific activity 1250 Ci × $mmol^{-1}$) was purchased from PerkinElmer, Inc. (Waltham, MA, USA). 5'-*N*-ethylcarboxamidoadenosine (NECA) was purchased from Sigma-Aldrich (Steinheim, Germany). N^6-cyclopentyladenosine (CPA) was purchased from Abcam (Cambridge, UK). Unlabeled ZM241385 was a gift from Dr. S.M. Poucher (Astra Zeneca, Macclesfield, UK). Adenosine deaminase (ADA) was purchased from Boehringer Mannheim (Mannheim, Germany). Bicinchoninic acid (BCA) and BCA protein assay reagent were obtained from Pierce Chemical Company (Rockford, IL, USA). Chinese hamster ovary cells stably expressing the hA_1AR ($CHOhA_1AR$) were provided by Prof. S.J. Hill (University of Nottingham, UK). Chinese hamster ovary cells stably expressing low levels of hA_1AR (CHO-hA_1AR-low) were obtained from Prof. Andrea Townsend (University College London, UK). HEK293 cells stably expressing the hA_{2A} adenosine receptor (HEK293 $hA_{2A}AR$) were kindly provided by Dr. J. Wang (Biogen/IDEC, Cambridge, MA, USA). Chinese hamster ovary cells stably expressing the human adenosine A_{2B} ($CHOhA_{2B}AR$) and A_3 receptor ($CHOhA_3AR$) were obtained from Dr. S. Rees (AstraZeneca, Macclesfield, UK) and Dr. K-N. Klotz (University of Würzburg, Germany), respectively. All other chemicals were of analytical grade and obtained from standard commercial sources.

2.3. Site-directed mutagenesis

Site-directed mutant hA_1AR-Y271F$^{7.36}$ was constructed by polymerase chain reaction mutagenesis using pcDNA3.1(+)-hA_1AR with N-terminal HA and C-terminal His tag as the template plasmid. Mutant primers for directional polymerase chain reaction product cloning were designed using the online QuikChange® Primer Design Program (Agilent Technologies, Santa Clara, CA, USA) and obtained from Eurogentec Nederland b.v. (Maastricht, The Netherlands). All DNA sequences were verified by Sanger sequencing at the Leiden Genome Technology Center (Leiden, The Netherlands).

2.4. Cell culture, transfection and membrane preparation

Cell culture and membranes preparation were performed as previously described [13,14].

2.5. Transient expression of wild type (WT) and mutant receptors in CHO cells

CHO cells were seeded into 150 mm culture dishes to achieve 50–60% confluence containing 20 mL of medium consisting of DMEM/F12 (1:1) supplemented with 10% (v/v) newborn calf serum, streptomycin (50 μg/mL), and penicillin (50 IU/mL). Cells were transfected approximately 24 h later with plasmid DNA (20 μg of DNA/dish) by the PEI method (PEI:DNA = 3:1) and left for 48 h [15]. Subsequently, medium was removed and fresh medium was added, and cells were grown for an additional 24 h at 37 °C and 5% CO_2. Membranes were prepared in the same way as previously described [13] and stored in 250 μL aliquots at −80 °C until further use.

2.6. Radioligand displacement assays

Adenosine A_1 Receptor [16]. Membrane aliquots containing 5 μg were incubated in a total volume of 100 μL assay buffer (50 mM Tris HCl, pH 7.4) at 25 °C for 60 min. Displacement experiments were performed using six concentrations of competing antagonist in the presence of ~1.6 nM [^{3}H]DPCPX. Nonspecific binding was determined in the presence of 100 μM CPA and represented < 10% of total binding. Incubation was terminated by rapid filtration performed on 96-well GF/B filter plates (Perkin Elmer, Groningen, the Netherlands) in a PerkinElmer Filtermate-harvester (Perkin Elmer, Groningen, the Netherlands) and washed with buffer (50 mM Tris-HCl, pH 7.4) After the filter plate was dried at 55 °C for 30 min, the filter-bound radioactivity was determined by scintillation spectrometry using a 2450 MicroBeta^2 Plate Counter (Perkin Elmer, Boston, MA).

Adenosine A_{2A} Receptor [14]. Membrane aliquots containing 20 μg of protein were incubated in a total volume of 100 μL of assay buffer (50 mM Tris-HCl, pH 7.4) at 25 °C for 120 min. Displacement experiments were performed using 1 μM of competing compound in the presence of ~2.5 nM [^{3}H]ZM241385. Nonspecific binding was determined in the presence of 100 μM NECA. Incubations were terminated, washed and samples were obtained and analysed as described under hA_1AR.

Adenosine A_{2B} Receptor [12]. Membrane aliquots containing 25 μg of protein were incubated in a total volume of 100 μL of assay buffer (50 mM Tris-HCl, pH 7.4, supplemented with 0.1% (w/v) CHAPS) at 25 °C for 120 min. Displacement experiments were performed using 1 μM of competing compound in the presence of ~1.5 nM [^{3}H]PSB-603. Nonspecific binding was determined in the presence of 10 μM ZM241385. Incubations were terminated, filters were washed with buffer (50 mM Tris-HCl, pH 7.4, supplemented with 0.1% BSA and 0.1% (w/v) CHAPS) and samples were obtained and analysed as described under hA_1AR.

Adenosine A_3 Receptor [17]. Membrane aliquots containing 15 μg of protein were incubated in a total volume of 100 μL of assay buffer (50 mM Tris-HCl, 10 mM $MgCl_2$, 1 mM EDTA, 0.01% CHAPS, pH 8.0) at 25 °C for 120 min. Displacement experiments were performed using 1 μM of competing compound in the presence of ~10 nM [^{3}H]PSB-11. Nonspecific binding was determined in the presence of 100 μM NECA. Incubations were terminated, washed with buffer (50 mM Tris-HCl, 10 mM $MgCl_2$, 1 mM EDTA, pH 8.0) and samples were obtained and analysed as described under hA_1AR.

2.7. Competition association assays

The binding kinetics of unlabelled ligands were assessed as described previously [16]. Briefly, the association of the radioligand was followed over time in the absence or presence of a concentration corresponding to IC_{50} value of unlabelled LUF7746 and LUF7747. In practice, to the mixture of equal volumes of 2.5 nM [^{3}H]DPCPX, unlabelled compound and assay buffer (50 mM Tris-HCl supplemented with 5 mM $MgCl_2$ and 0.1% CHAPS) was added a 25 μL membrane aliquot containing 5 μg of protein at each time point from 0.5 min to 240 min at 25 °C. Incubation was terminated as described above (radioligand displacement assay).

2.8. Wash-out assay on both wild type hA_1AR and hA_1AR-Y271F$^{7.36}$ cell membranes

100 μL of assay buffer containing either 1% DMSO (blank control) or 1 μM of ligands (LUF7746 or LUF7747) and 200 μL additional assay buffer were added to a 2 mL Eppendorf tube containing 100 μL cell membrane suspension (20 μg and 40 μg of protein for WT and Y271F$^{7.36}$, respectively, to obtain an assay window of 3000 dpm in both cases) to achieve a total volume of 400 μL. The tubes were incubated for 2 h in an Eppendorf® Thermomixer® at 900 rpm and 25 °C. After incubation the tubes were centrifuged for 5 min at 16,000 × *g* and 4 °C and subsequently the buffer, containing unbound ligands, was removed. The membrane pellet was resuspended in 1 mL of assay buffer, incubated for 10 min at 25 °C and 900 rpm after which the tubes were centrifuged for 5 min at 16,000 × *g* and 4 °C and the cycle was repeated three more times. After the final washing step, the membrane pellet was resuspended in 300 μL assay buffer to determine the radioligand binding activity. All samples were transferred to the test tubes and incubated with 100 μL of 1.6 nM [^{3}H]DPCPX for 2 h at 25 °C. The incubation was terminated by vacuum filtration through a GF/B filter using a Brandel M24 Scintillation Harvester to separate bound and free radioligand. The filters were washed three times with ice-cold wash buffer (50 mM Tris-HCl, pH 7.4). After drying the filters, 3.5 mL of scintillation liquid was added and the filter-bound radioactivity was determined in a Tri-Carb 2900TR Liquid Scintillation Analyzer (PerkinElmer, Inc., Waltham, MA, USA). Results are expressed as percentage normalized to the maximum specific binding in the control group (100%).

2.9. Computational modelling

All calculations were performed using the Schrödinger Suite [18]. The X-ray structure of the hA_1AR was extracted from the PDB (PDB: 5UEN) [19,20]. The co-crystalized ligand DU172 was removed and protein chain A was prepared for docking with the Protein Preparation tool. Additionally, missing side chains were added using Prime [21].

2.10. Functional [^{35}S]GTPγS binding assay

Binding of [^{35}S]GTPγS to membranes was adapted from a previously reported method [22]. The assays were performed in a 96-well plate format, where stock solutions of the compounds were added using an HP D300 Digital Dispenser (Tecan, Männedorf, Switzerland). The final concentration of DMSO per assay point was ≤0.1%. For concentration–response assays, transiently transfected membranes (hA_1AR-WT, 5 μg and hA_1AR-Y271F$^{7.36}$, 20 μg to obtain an assay window of 3000 dpm in both cases) in 80 μL total volume of assay buffer containing 50 mM Tris-HCl buffer, 5 mM $MgCl_2$, 1 mM EDTA, 100 mM NaCl, 0.05% BSA and 1 mM DTT pH 7.4 supplemented with 3 μM GDP and saponin (hA_1AR-WT, 5 μg and hA_1AR-Y271F$^{7.36}$, 20 μg) were added to a range of concentrations of ligand (10^{-10} to 10^{-5}) for 30 min at 25 °C. After this, 20 μL of [^{35}S]GTPγS (final concentration of 0.3 nM) was added and incubation continued for another 90 min at 25 °C. The basal level of [^{35}S]GTPγS binding was determined in the absence of ligand, whereas the maximal level of [^{35}S]GTPγS binding was determined in the presence of 1 μM CPA. For receptor activation/inhibition studies, hA_1AR-WT or hA_1AR-Y271F$^{7.36}$ cell membranes were pre-incubated with LUF7746 or LUF7747 (EC_{80} concentration) for 60 min. After this, [^{35}S]GTPγS (final concentration of 0.3 nM) was added in the absence or presence of DPCPX (1 μM) for another 90 min. For all experiments, incubations were terminated by rapid vacuum filtration to separate the bound and free radioligand through Whatman™ UniFilter™ 96-well GF/B microplates using a PerkinElmer's FilterMate™ Universal Harvester (PerkinElmer, Groningen, Netherlands). Filters were subsequently washed three times with 2 mL of ice-cold buffer (50 mM Tris-HCl, pH 7.4 supplemented with 5 mM $MgCl_2$). The filter-bound radioactivity was determined by scintillation spectrometry using a PerkinElmer MicroBeta2 2450 Microplate Counter (PerkinElmer, Groningen, Netherlands).

2.11. Label-free whole-cell assays

Label-free whole-cell assays were adapted from a previously reported method [23,24] using the real-time cell analyser (RTCA) xCELLigence SP system (ACEA Biosciences, San Diego, CA, USA) [24]. The system measures electrical impedance generated by adherence of cells

to gold-coated electrodes at the bottom of 96 wells PET E-plates (obtained from Bioké, Leiden, the Netherlands). Changes in impedance (Z) were measured continuously and are displayed as Cell Index (CI), which is defined as ($Z_i - Z_0$) Ω/15 Ω. Z_i is the impedance at a given time and Z_0 is the baseline impedance measured at the start of the experiment in the absence of cells. CHO cells stably expressing a relatively low level hA_1AR (CHO-hA_1AR-low) were cultured in medium of DMEM/F12 (1:1) supplemented with 10% (v/v) newborn calf serum, streptomycin (50 μg/mL), penicillin (50 IU/mL), and G418 (0.2 mg/mL) at 37 °C in 5% CO_2 as a monolayer on 10 cm ø culture plates to 70–80% confluency and subsequently harvested and centrifuged twice at 200*g* for 5 min [25]. Initially, 60 μL of culture medium was added to wells in E-plates 96 to obtain background readings (Z_0) followed by the addition of 40 μL of cell suspension containing 40,000 cells per well. After resting at room temperature for 30 min, the plate was mounted in the RTCA recording station within a humidified 37 °C, 5% CO_2 incubator. Impedance was measured every 15 min overnight. For agonist assays, after 17 h, medium was replaced with 95 μL serum free medium plus 1.2 IU ADA and kept in the 37 °C, 5% CO_2 incubator for 3 h of starvation. After that, cells were stimulated with increasing concentrations of agonists or vehicle (final concentration of 0.25% DMSO) in a final well volume of 100 μL. For the inverse agonist reversal assay, cells were placed in 90 μL serum free medium containing 1.2 IU/ml ADA for 3 h starvation. Then cells were stimulated with 5 μL indicated compound (final concentration 1 μM) for 30 min, followed by the addition of 100 nM DPCPX in a final well volume of 100 μL. For both assays, to record the signal changes, CI was recorded for at least 30 min with a recording schedule of 15 s intervals for 20 min, followed by intervals of 1 min, 5 min and finally 15 min. For data analysis, the individual CI traces were normalized, by subtracting the baseline (vehicle control), to correct for any agonist-independent signals.

2.12. Data analysis

All the experimental data were analysed with GraphPad Prism 7.0 software (GraphPad Software Inc., San Diego, CA). pIC_{50} values in radioligand displacement assays were obtained by non-linear regression curve fitting into a sigmoidal concentration–response curve using the "log(inhibitor) vs. response" GraphPad Prism analysis equation. pK_i values were obtained from pIC_{50} values using the Cheng–Prusoff equation [26]. A K_D value of 1.6 nM for [^{3}H]DPCPX was used on the $CHOhA_1AR$, as previously determined [28]. Association data for the radioligand were fitted using one-phase exponential association. Values for k_{on} were obtained by converting k_{obs} values using the following equation: $k_{on} = (k_{obs} - k_{off})/[\text{radioligand}]$, where k_{off} values (0.21 ± 0.01 min^{-1}) were cited from Guo *et al.* [16]. Association and dissociation rates for unlabelled ligands were calculated by fitting the data in the competition association model using 'kinetics of competitive binding' [16,27].

$$K_A = k_1[L]\cdot 10^{-9} + k_2$$
$$K_B = k_3[I]\cdot 10^{-9} + k_4$$
$$S = \sqrt{(K_A - K_B)^2 + 4\cdot k_1\cdot k_3\cdot L\cdot I\cdot 10^{-18}}$$
$$K_F = 0.5(K_A + K_B + S)$$
$$K_S = 0.5(K_A + K_B - S)$$
$$Q = \frac{B_{max}\cdot k_1\cdot L\cdot 10^{-9}}{K_F - K_S}$$
$$Y = Q\cdot\left(\frac{k_4\cdot(K_F - K_S)}{K_F\cdot K_S} + \frac{k_4 - K_F}{K_F}e^{(-K_F\cdot X)} - \frac{k_4 - K_S}{K_S}e^{(-K_S\cdot X)}\right)$$

Herein, X is the time (min), Y is the specific [^{3}H]DPCPX binding (dpm), k_1 and k_2 are the k_{on} and k_{off} of [^{3}H]DPCPX and were obtained from Guo *et al.* [16], L is the concentration of [^{3}H]DPCPX used (nM), B_{max} the total binding (dpm) and I the concentration of unlabelled ligand (nM). Fixing these parameters allows the following parameters to be calculated: k_3, which is the k_{on} value (M^{-1} min^{-1}) of the unlabelled ligand and k_4, which is the k_{off} value (min^{-1}) of the unlabelled ligand. The residence time (RT) was calculated using $RT = 1/k_{off}$. pEC_{50} and EC_{80} values in the [^{35}S]GTPγS binding assays were determined using non-linear regression curve fitting into a sigmoidal dose–response curve with variable slope. For the label-free whole-cell assays, ligand responses were normalized to obtain normalized cell index (NCI) and then subtracted baseline (vehicle control), which correct for ligand-independent effects. Area-under-curve (AUC) values from the NCI were determined for a 100 min period after compound addition, which were used for concentration–response curves. pEC_{50} values from the label-free whole-cell assays were determined using the same non-linear regression as for the [^{35}S]GTPγS binding assays. Data shown represent the mean ± SEM of three individual experiments each performed in duplicate or a representative graph is shown. Statistical analysis was performed as indicated. If p values were below 0.05, observed differences were considered statistically significant.

3. Results

3.1. Design and synthesis of LUF7746 and LUF7747

Over the years our research group has explored a series of hA_1AR agonists based on the 6-amino-4-aryl-3,5-dicyano-2-thiopyridine scaffold, to investigate their structure–activity and structure-kinetics relationships (SAR and SKR) [9,28]. We learned that the benzo[1,3]dioxol-5-yl moiety generally provided selective and potent agonists for hA_1AR. Based on that finding, we used 2-amino-4-(benzo[*d*][1,3]dioxol-5-yl)-6-mercaptopyridine-3,5-dicarbonitrile as a scaffold (Fig. 1), and developed a potentially covalent ligand by incorporating the fluorosulfonyl moiety as a warhead through an amide linker at the position of the sulphur atom. Hence, LUF7746, 4-((3-((6-amino-4-(benzo[*d*][1,3]dioxol-5-yl)-3,5-dicyanopyridin-2-yl)thio)propyl)carbamoyl)benzenesulfonylfluoride (Fig. 1), was synthesized in one step by alkylating the scaffold with the corresponding alkyl bromide. Additionally, the reactive fluorosulfonyl warhead was replaced with a methylsulfonyl moiety, which yielded a nonreactive control compound, *N*-(3-((6-amino-4-(benzo[*d*][1,3]dioxol-5-yl)-3,5-dicyanopyridin-2-yl)thio)propyl)-4-(methylsulfonyl)benzamide (LUF7747, Fig. 1).

3.2. Characterization of LUF7746 as a covalent probe

3.2.1. Affinity characterization of LUF7746 and LUF7747 at different incubation times

To determine the affinity of the synthesized ligands we tested both ligands in a [^{3}H]DPCPX displacement assay at 25 °C. After 0.5 h co-incubation time, both compounds were able to concentration-dependently inhibit specific [^{3}H]DPCPX binding to the hA_1AR (Fig. 2). As presented in Table 1, both compounds showed similar binding affinities in the submicromolar range (pK_i = 7.7 ± 0.1 and 7.2 ± 0.04 for LUF7746 and LUF7747, respectively). We then tested the time dependency of the affinity for both compounds. In detail, the CHO cell membranes overexpressing hA_1AR were pre-incubated with the indicated compound for 4 h, followed by a 0.5 h co-incubation with the radioligand [^{3}H]DPCPX. LUF7746 showed a significantly increased affinity with 4 h preincubation time (pK_i = 8.4 ± 0.1; Table 1), while LUF7747's affinity did not change (pK_i = 7.3 ± 0.02; Table 1). Representative graphs for this effect are shown in Fig. 2, in which the curve representing a concentration-dependent inhibition of specific [^{3}H]DPCPX binding was shifted to the left with 4 h pre-incubation of LUF7746 (Fig. 2a), with no difference for LUF7747 (Fig. 2b). It is worth to mention that for a covalent ligand no dynamic equilibrium can be reached. We thus expressed LUF7746's affinity for hA_1AR as "apparent K_i". Compared to the reversible ligand LUF7747, covalent LUF7746 showed an increase in apparent pK_i with 0.7 log unit. The increased receptor affinity by LUF7746 with prolonged incubation time, indicated an increased level of covalent, non-displaceable binding over time.

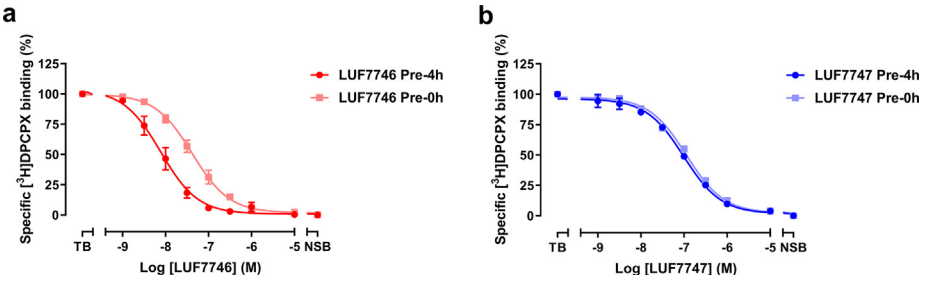

Fig. 2. Affinity assessment of LUF7746 and LUF7747 at different incubation time. Displacement of specific [^{3}H]DPCPX binding from the cell membranes stably expressing hA$_1$AR at 25 °C by LUF7746 (a), and LUF7747 (b) with or without a pre-incubation of 4 h. Data are normalized to 100% of the total binding and represent the mean ± SEM of at least three individual experiments performed in duplicate.

Additionally, we tested these compounds in a single-point radioligand binding assay for other adenosine receptor subtypes (Table 1). Both compounds displaced < 50% of the total radioligand binding at 1 μM for other subtypes of human adenosine receptors (i.e. yielding estimated IC_{50} values higher than 1 μM), even when the incubation time was doubled. Thus, both ligands are selective towards the hA$_1$AR.

3.2.2. Characterization of the binding kinetics of LUF7746 and LUF7747

The apparent affinity shift of LUF7746 inspired us to examine the kinetic characteristics of the ligand-receptor interaction and to investigate the ligand's dissociation rate. In our previous research, the kinetic binding parameters k_{on} (k_1 = 1.2 ± 0.1 × 10^8 M^{-1} min^{-1}) and k_{off} (k_2 = 0.23 ± 0.01 min^{-1}) of [^{3}H]DPCPX at 25 °C had been determined in traditional association and dissociation assays [16,27,29]. In this study we derived the kinetic binding parameters for the two unlabelled ligands by performing a competition association assay at a concentration of their IC_{50} value. The association in the presence of LUF7747 (Fig. 3) reached a plateau within 30 min, indicating a dynamic equilibrium was reached between [^{3}H]DPCPX, ligand and hA$_1$AR. Following the (equilibrium) Motulsky and Mahan model [27], we calculated an association rate constant of 6.3 ± 0.9 × 10^6 M^{-1} min^{-1} and a fast dissociation rate constant (0.42 ± 0.03 M^{-1} min^{-1}) which equalled to a receptor residence time (RT) of 2.4 ± 0.3 min for reversible ligand LUF7747. Interestingly, LUF7746's behaviour caused an initial 'overshoot' of [^{3}H]DPCPX binding in the competition association curve which decreased over time (Fig. 3). As no equilibrium between receptors and ligand was reached for LUF7746, the kinetic parameters cannot be analysed according to the Motulsky and Mahan model [27]. These data provided further evidence for a putative irreversible binding mode between LUF7746 and the hA$_1$AR.

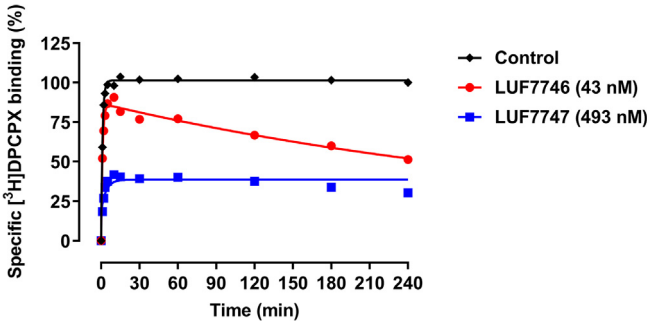

Fig. 3. Characterization of target binding kinetics of LUF7746 and LUF7747. Competition association radioligand binding assay with [^{3}H]DPCPX in the absence or presence of indicated compounds (at IC_{50} value) at 25 °C. Data were fitted to the equations described in the methods to calculate the k_{on} (k_3) and k_{off} (k_4) values of unlabelled ligands by using the k_{on} (k_1) and k_{off} (k_2) values of [^{3}H]DPCPX. Kinetic parameters of LUF7747 were obtained from combined graphs of multiple experiments (n = 4). Representative graph from one experiment performed in duplicate.

3.2.3. Determination of the wash-resistance of LUF7746 and LUF7747

Subsequently, a "washout" experiment was performed to investigate the irreversibility of the ligand-receptor interaction. We first exposed hA$_1$AR cell membranes to LUF7746 or LUF7747 at 1 μM concentration with [^{3}H]DPCPX for 2 h, without any washing step, to assess the binding capacity of the receptor ("unwashed" group; Fig. 4a). Both ligands achieved a high receptor occupancy, resulting in a lower radioligand-occupied receptor population of 23 ± 2% for LUF7746 and 38 ± 4% for LUF7747, respectively. For the "washed" groups, the pre-incubated hA$_1$AR membranes were washed four times to remove the non-covalently bound ligands ("washed" group; Fig. 4a), after which they were exposed to [^{3}H]DPCPX. Membranes pre-treated with

Table 1
Binding affinities of LUF7746 and LUF7747 for all adenosine receptor subtypes and mutant hA$_1$AR-Y271F$^{7.36}$.

	pK_i[a] (pre-0 h)	pK_i[b] (pre-4 h)	Displacement at 1 μM (%)			pIC_{50}
Compound	hA$_1$AR		hA$_{2A}$AR[c]	hA$_{2B}$AR[d]	hA$_3$AR[e]	hA$_1$AR-Y271F$^{7.36}$[f]
LUF7746[g]	7.7 ± 0.1	8.4 ± 0.1**	33 ± 8	15 ± 11	28 ± 6	7.2 ± 0.05
LUF7747	7.2 ± 0.04	7.3 ± 0.02	14 ± 3	12 ± 5	11 ± 5	7.0 ± 0.06

Values represent pK_i ± SEM (n = 3) or mean percentage displacement at 1 μM (n = 3) of individual experiments each performed in duplicate.

** $p < 0.01$ compared with the pK_i values in displacement experiments without pre-incubation; Student's *t*-test.

[a] Affinity determined from displacement of specific [^{3}H]DPCPX binding on CHO cell membranes stably expressing hA$_1$AR at 25 °C after 0.5 h co-incubation;

[b] Affinity determined from displacement of specific [^{3}H]DPCPX binding on CHO cell membranes stably expressing hA$_1$AR at 25 °C with compounds pre-incubated for 4 h, followed up by a 0.5 h co-incubation with [^{3}H]DPCPX;

[c] % displacement at 1 μM concentration of specific [^{3}H]ZM241385 binding on HEK293 cell membranes stably expressing human adenosine A_{2A} receptors at 25 °C after 2 h co-incubation;

[d] % displacement at 1 μM concentration of specific [^{3}H]PSB-603 binding on CHO cell membranes stably expressing human adenosine A_{2B} receptors at 25 °C after 2 h co-incubation;

[e] % displacement at 1 μM concentration of specific [^{3}H]PSB-11 binding on CHO cell membranes stably expressing human adenosine A_3 receptors at 25 °C after 2 h co-incubation;

[f] Affinity determined from displacement of specific [^{3}H]DPCPX binding on CHO cell membranes transiently expressing hA$_1$AR-Y271F$^{7.36}$ at 25 °C after 2 h co-incubation ;

[g] For LUF7746, affinity values can only be apparent, as true equilibrium cannot be reached.

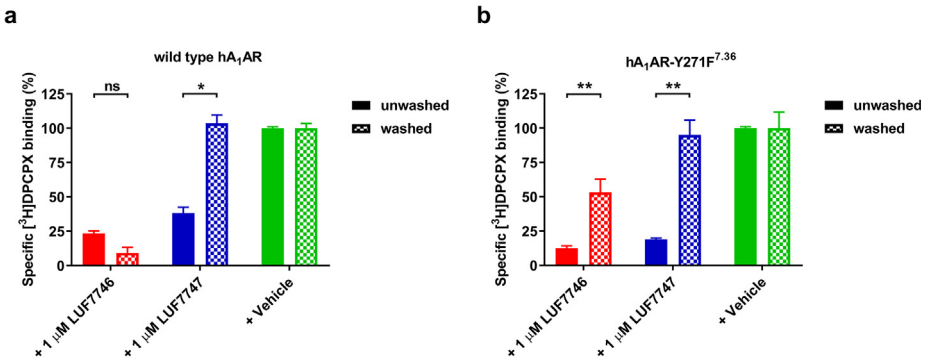

Fig. 4. Anchor point characterization by washout assay. CHOhA_1AR cell membranes (a) or CHO cell membranes transiently expressing mutant hA_1AR-$Y271F^{7.36}$ (b) were pre-treated with 1 μM LUF7746, LUF7747 or buffer (vehicle) followed by no washing (filled column) or four washing cycles (chequered column). The membranes were then subjected to a standard [^{3}H]DPCPX radioligand binding assay. Data are expressed as the percentage of vehicle group (100%) and represent mean ± SEM of three individual experiments performed in duplicate. Statistical analyses were performed using unpaired Student's *t*-test between groups. ns: no significant difference; Significant difference: $^*p < 0.05$; $^{**}p < 0.01$.

LUF7746 showed no increase in specific [^{3}H]DPCPX binding with only 9 ± 4% recovery despite the intensive washing treatment. In contrast, membranes pre-treated with LUF7747 showed a full recovery of radioligand binding (104 ± 6%), ensuring the efficiency of the washing procedure to remove the reversible ligand.

3.2.4. Functional characterization of LUF7746 and LUF7747 in a [^{35}S]GTPγS binding assay

To extend the functional profiling of what emerged from the data presented above from the radioligand binding assays, we evaluated the compounds' functional activities in a GTPγS-binding assay on CHO cell membranes transiently transfected with wild type hA_1AR (hA_1AR-WT). This assay reflects the functional response of ligands at the level of GDP/GTP exchange by the ternary G protein complex, or G protein activation [30].

The results showed that LUF7746 and LUF7747 are both partial agonists with an E_{max} of 56 ± 5% and 53 ± 2% respectively (Fig. 5a; Table 2), compared to the response obtained at a concentration of 1 μM CPA, a reference full agonist with a pEC_{50} value of 8.1 ± 0.1. The potency and (apparent) affinity of LUF7746 (pEC_{50} = 7.4 ± 0.1; Table 2, pK_i = 7.7 ± 0.1; Table 1) and LUF7747 (pEC_{50} = 7.2 ± 0.02; Table 2, pK_i = 7.2 ± 0.04; Table 1) were all in the double digit nanomolar range.

To investigate the irreversible agonistic effect of LUF7746, we added inverse agonist DPCPX to hA_1AR-WT pre-incubated with the designed agonist at EC_{80} concentration. Although not significant, in the absence of agonist pre-incubation, DPCPX showed a minimal reduction in the basal level of G protein activity (−4 ± 1%; Fig. 5c), consistent with an inverse agonistic behaviour. Moreover, the G protein activation induced by LUF7746 and LUF7747 at EC_{80} concentration was inhibited by subsequent addition of DPCPX to varying degrees. Specifically, LUF7747 stimulation of G protein activity was completely reversed (−4 ± 2%; Fig. 5c), to an extent that was also obtained by treatment with DPCPX alone (−4 ± 1%; Fig. 5c). [^{35}S]GTPγS binding upon LUF7746 stimulation was only slightly reversed by DPCPX (83 ± 2%; Fig. 5c), possibly due to the fact that not all receptors are irreversibly labelled by LUF7746 at an EC_{80} concentration.

Table 2
Functional characterization of LUF7746 and LUF7747 in [^{35}S]GTPγS binding assays.

Compound	CHOhA_1AR-WT		CHOhA_{1A}R-$Y271F^{7.36}$	
	pEC_{50}	E_{max} (%)[a]	pEC_{50}	E_{max} (%)[b]
CPA	8.1 ± 0.1	100 ± 13	8.4 ± 0.03	100 ± 4
LUF7746	7.4 ± 0.1	56 ± 5*	6.8 ± 0.1	66 ± 1***
LUF7747	7.2 ± 0.02	53 ± 2*	7.1 ± 0.1	66 ± 5***

Values represent the mean ± SEM of three individual experiments each performed in duplicate.

[a] Expressed as percentage of [^{35}S]GTPγS binding induced by 1 μM CPA (set at 100%).

* $p < 0.05$, compared to CPA using one-way ANOVA with Dunnett's post-test.

[b] Expressed as percentage of [^{35}S]GTPγS binding induced by 1 μM CPA (set at 100%).

*** $p < 0.001$, compared to CPA using one-way ANOVA with Dunnett's post-test.

3.3. Prediction of the binding mode of LUF7746 in the hA_1AR binding pocket

The characterization of the irreversible binding nature between LUF7746 and hA_1AR prompted us to further investigate the target residue of the reactive warhead. Thus, we first retrieved the receptor atomic coordinates from a reported hA_1AR X-ray crystal structure (PDB: 5UEN) [19] and constructed a receptor model in which hA_1AR and LUF7746 interact. The binding pose of LUF7746 (Fig. 6), is comparable to that of DU172, the ligand present in the crystal structure. Specifically, one cyano group at the C^5 position participated in H-bond formation with the amide of $N254^{6.55}$. The dioxomethylene substituent functioned as H-bond acceptor with $T91^{3.36}$, while carbonyl-oxygen in the amide position of the linker hydrogen-bonded with $N70^{2.65}$. Of note, the flexibility of the three carbon linker allowed the warhead, the fluorosulfophenyl group of LUF7746, to form a covalent sulfonyl amide bond with the phenolic hydroxyl group of $Y271^{7.36}$.

3.4. Determination of tyrosine residue $Y271^{7.36}$ as possible anchor point for covalent bond formation

To verify this structural feature of the ligand-receptor interaction, we mutated the potential target tyrosine to phenylalanine (hA_1AR-$Y271F^{7.36}$) and determined the affinities of both ligands for the mutant construct. As presented in Table 1, both compounds showed similar binding affinities in the submicromolar range (pIC_{50} = 7.2 ± 0.05 and 7.0 ± 0.06 for LUF7746 and LUF7747, respectively). Subsequently, we repeated the "washout" assay. As shown in Fig. 4b, washing of the mutant membranes, preincubated with LUF7746, caused a significant recovery in [^{3}H]DPCPX binding (53 ± 10% remaining) compared to the unwashed group (12 ± 2%). This significant recovery was in striking contrast to the washout assay on hA_1AR-WT, which showed no recovery at all (Fig. 4a). As a control, LUF7747 was rapidly washed off the membranes overexpressing hA_1AR-$Y271F^{7.36}$, as a full recovery of radioligand binding was observed (95 ± 11%).

In addition to the radioligand binding assay, potency and efficacy of both ligands were also evaluated in a GTPγS-binding assay on cell membranes transiently transfected with hA_1AR-$Y271F^{7.36}$. Both LUF7746 and LUF7747 showed a comparable E_{max} value (66 ± 1% and 66 ± 5%; Fig. 5b; Table 2) compared to reference full agonist CPA that had a pEC_{50} value of 8.4 ± 0.03 (maximum response E_{max} set to 100%, at a concentration of 1 μM). This indicates that the two compounds are still partial agonists on mutant hA_1AR-$Y271F^{7.36}$ receptors. The potency of LUF7746 was slightly decreased on hA_1AR-$Y271F^{7.36}$

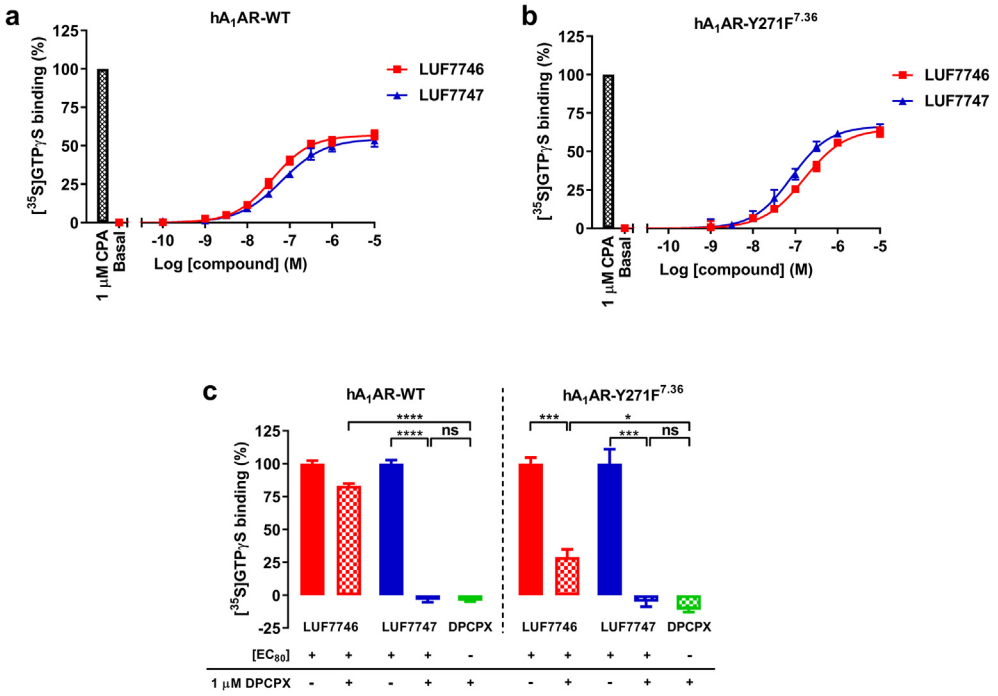

Fig. 5. Functional characterization of LUF7746 and LUF7747 in [^{35}S]GTPγS binding assays on both hA$_1$AR-WT and hA$_1$AR-Y271F$^{7.36}$. (a) Functional ([^{35}S]GTPγS binding) concentration-effect curves for CPA, LUF7746 and LUF7747 on transiently transfected hA$_1$AR-WT cell membranes. Data are expressed as percentage of the response induced by 1 μM CPA (100%) and represent the mean ± SEM of three individual experiments performed in duplicate. (b) Functional ([^{35}S]GTPγS binding) concentration-effect curves for CPA, LUF7746 and LUF7747 on transiently transfected hA$_1$AR-Y271F$^{7.36}$ cell membranes. Data are expressed as percentage of the response induced by 1 μM CPA (100%) and represent the mean ± SEM of three individual experiments performed in duplicate. Parameters obtained from these graphs are described in Table 2. (c) hA$_1$AR-WT or hA$_1$AR-Y271F$^{7.36}$ cell membranes were pre-incubated with LUF7746 or LUF7747 (EC$_{80}$, obtained from Fig. 5a or b) for 1 h, followed by incubation with [^{35}S]GTPγS in the absence (filled columns) or presence (chequered columns) of DPCPX (1 μM) to determine residual [^{35}S]GTPγS binding. Data are expressed as percentage of the response induced by LUF7746 or LUF7747 at EC$_{80}$ (100%) and represent the mean ± SEM of three individual experiments performed in duplicate. Statistical analyses were performed using unpaired Student's *t*-test between groups. ns: no significant difference; Significant difference: $*p < 0.05$; $***p < 0.005$; $****p < 0.001$.

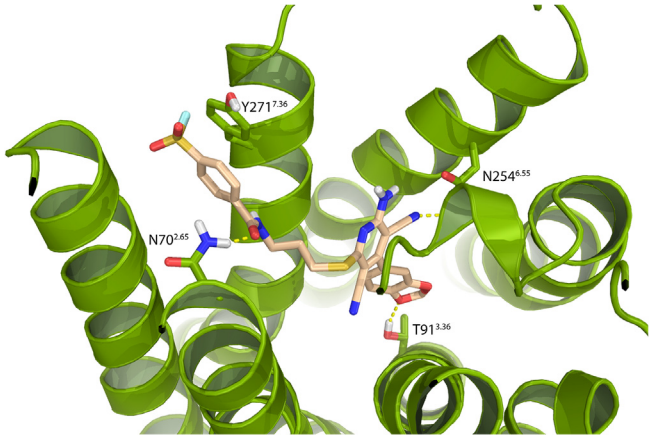

Fig. 6. Prediction of LUF7746's binding mode in the hA$_1$AR-binding pocket. The binding mode of LUF7746 was modelled in the ligand binding pocket present in the hA$_1$AR crystal structure (PDB: 5UEN). Receptor helices are represented in green with several amino acids marked. LUF7746 is represented by light brown carbon sticks, together with oxygen, nitrogen, sulphur and hydrogen atoms (coloured red, blue, yellow and white, respectively). The hydrogen bonds between ligand and receptor are indicated by yellow dashed lines. The ligand's fluorosulfonyl group and Y271$^{7.36}$ are in close proximity to facilitate covalent bond formation. (For interpretation of the references to colour in this figure legend, the reader is referred to the web version of this article.)

(pEC$_{50}$ = 6.8 ± 0.1; Fig. 5b, Table 2) compared to hA$_1$AR-WT (pEC$_{50}$ = 7.4 ± 0.1; Fig. 5a, Table 2), while the potency value of LUF7747 was identical between hA$_1$AR-Y271F$^{7.36}$ (pEC$_{50}$ = 7.1 ± 0.1; Fig. 5b, Table 2) and hA$_1$AR-WT (pEC$_{50}$ = 7.2 ± 0.02; Fig. 5a, Table 2). Then on hA$_1$AR-Y271F$^{7.36}$, we repeated the DPCPX inhibition experiments on cell membranes pre-treated with both LUF7746 and LUF7747 at EC$_{80}$ concentration. As shown in Fig. 5c, DPCPX caused a more pronounced effect to reverse the stimulation of [^{35}S]GTPγS binding induced by LUF7746 (29 ± 6%) on the mutant membranes, compared to the inhibition on hA$_1$AR-WT (83 ± 2%). As a control, LUF7747's stimulation on hA$_1$AR-Y271F$^{7.36}$ was completely reversed (−5 ± 4%), comparable to the group only treated with DPCPX (−11 ± 2%).

3.5. Characterization of the covalent interaction in a label-free whole cell assay

To further evaluate receptor activation by these ligands, we used a label-free, impedance-based technology (xCELLigence) capable of real-time monitoring of hA$_1$AR-mediated cell morphological changes over time [24]. Typically, CHO cells stably expressing a relative low level of hA$_1$AR (CHO-hA$_1$AR-low) were plated on an E-plate 17 h before the experiment [31]. Upon agonist addition to these cells, the impedance (shown as cell index, CI) was dose-dependently increased, followed by a gradual decrease until reaching a plateau in most cases after 100 min. A representative experiment of CPA-induced impedance changes is shown in Fig. 7a. Dose-response curves for CPA and the two LUF compounds were derived from the area under curve (AUC) of corresponding agonist-induced changes within 100 min (Fig. 7b). Specifically, compared to CPA, LUF7746 and LUF7747 again behaved as partial agonists with similar E$_{max}$ values and potencies (see Fig. 7b and Table 3).

To probe the putative irreversibility of the designed agonist, we used this label-free assay to determine whether the activation of the receptor is reversed by subsequent addition of the A$_1$AR antagonist/inverse agonist DPCPX (i.e. similar to the GTPγS experiments with membranes). After the CHO-hA$_1$AR-low cells were incubated with compounds for 30 min DPCPX (100 nM) or 0.25% DMSO (vehicle) was added and the impedance change was measured until 100 min. As shown in Fig. 8a, cells exposed to LUF7746 showed a slight drop of CI values with a recovery trend back to control (0.25% DMSO). A more pronounced decrease of CI was detected upon antagonist exposure of cells pre-treated with LUF7747 (Fig. 8b). This behaviour showed that LUF7746-pretreated cells were quite resistant to DPCPX compared to LUF7747, consistent with an irreversible mode of receptor activation.

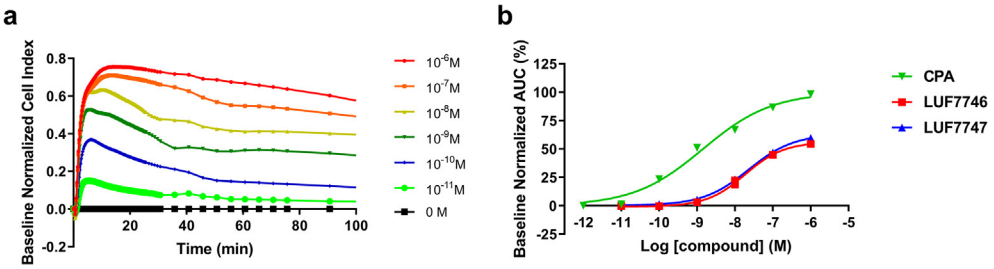

Fig. 7. Functional characterization of CPA, LUF7746 and LUF7747 in a label-free whole cell assay. CHO-hA_1AR-low cells were seeded into a 96 wells E-plate (40,000 cells/well) for 17 h, followed by 3 h serum-free medium plus ADA (1.2 IU/ml) starvation, prior to the indicated agonist treatment. (a) Representative example of a baseline-corrected CPA response [1 μM–10 pM]. (b) Concentration-response curves of the three agonists, derived from similar curves as in (a). Parameters obtained from these graphs are listed in Table 3. Data are expressed as the percentage of maximal response induced by 1 μM CPA (analysis of area-under-curve (AUC) at 100 min, 100%) and represent mean ± SEM of three individual experiments performed in duplicate.

Table 3
Pharmacological characterization of LUF7746 and LUF7747 in a label-free whole-cell assay.

Compound	CHO-hA_1AR-low cells	
	pEC_{50}	E_{max} (%)[a]
CPA	8.9 ± 0.06	100 ± 7
LUF7746	7.7 ± 0.1	61 ± 1**
LUF7747	7.6 ± 0.03	69 ± 4**

Values represent the mean ± SEM of three individual experiments performed in duplicate.

[a] Data were normalized to the CPA response at 1 μM (100%).

** $p < 0.01$, compared to CPA efficacy (E_{max}) response using one-way ANOVA with Dunnett's post-test.

4. Discussion

Covalent ligands have been invaluable in the study of ligand-receptor interactions and in GPCR structural biology. Recently, several GPCR structures, such as cannabinoid CB_1 receptor [32] and adenosine A_1 receptor [19], have been determined in the presence of chemo-reactive ligands contributing to the formation of stable and functional ligand-receptor complexes. More generally, the use of covalent affinity probes for the exploration of the ligand binding pocket is widespread in GPCR research [2].

The non-ribose agonists' design dates back to the discovery of a former drug candidate, capadenoson, withdrawn from phase IIa clinical studies when it failed to show heart rate reduction for patients with atrial fibrillation [10,11]. The structure modifications in capadenoson derivatives revealed that the dicyanopyridine scaffold with a benzo [1,3]dioxol-5-yl moiety at the C^4 position showed good selectivity and efficacy at the hA_1AR [9,28]. Building on that, we introduced a reactive warhead (i.e. fluorosulfonyl), connected to the scaffold's atom with an amide bond linked spacer, yielding the covalent dicyanopyridine ligand LUF7746. Additionally, a nonreactive methylsulfonyl derivative LUF7747, was designed and synthesized as a reversible control compound.

The first hint of covalent interaction of LUF7746 was found in time-dependent radioligand displacement assays, while the control ligand LUF7747 reached equilibrium independent of pre-incubation time. Similar experiments were performed on other subtypes of GPCRs, such as the M_4 muscarinic receptor and cannabinoid CB_1 receptor. All of the functionalized covalent ligands generated a time-dependent affinity increase [33,34]. Subsequently, a continuing decrease of specific radioligand binding was observed for LUF7746 when the kinetic experiments were performed over a 4 h incubation at 25 °C (Fig. 3). A similar trend in competition association experiments was found for the irreversible hA_1AR antagonist FSCPX [35]. Therefore, these results further indicate an irreversible interaction between the receptor and LUF7746 in contrast to the reversible binding of LUF7747 for which an equilibrium was observed resulting in a short RT of 2.4 ± 0.3 min. The inadequacy of the Motulsky and Mahan model to fit this data is further evidence for the non-equilibrium features of the binding of LUF7746 to the receptor. In addition, extensive washing failed to restore [^{3}H] DPCPX binding (Fig. 4a) to membranes pre-treated with LUF7746, validating the irreversible nature of LUF7746 to hA_1AR. Likewise, on other GPCR subtypes, there are reported cases showing a covalent interaction was wash-resistant [14,36,37]. Furthermore, receptor activation induced by LUF7746 was not or hardly inhibited by the inverse agonist DPCPX (Fig. 5c). This confirmed the covalent nature of LUF7746 binding to the receptor from a functional perspective, similar to other subtypes of GPCRs, where an excess of inverse agonist was unable to reverse covalent ligand-induced G protein activation [38]. Taking all data together we concluded LUF7746 shows a covalent interaction with hA_1AR under many different experimental conditions.

The next step was to identify the anchor point of the covalent probe. The reported active structure of the hA_1AR is in the presence of the ribose-based full agonist adenosine, which is structurally and functionally distinct from our non-ribose partial agonist LUF7746 [39]. In addition, our previous study on the dicyanopyridine scaffold showed that upon the addition of GTP this compound class only caused a minor shift to a lower affinity on hA_1AR [40]. It is thus possible that this non-ribose partial agonist-bound receptor adopts a conformation distinct from the fully active state. Therefore, we adopted the inactive state of the hA_1AR receptor (PDB: 5UEN) for our docking studies [19]. Based on the LUF7746 binding pose in our model of the hA_1AR, we hypothesized that LUF7746 covalently interacts with a tyrosine residue, $Y271^{7.36}$, resulting in a sulfonate bond formation (Fig. 6).

To investigate our hypothesis, this tyrosine was mutated to phenylalanine (hA_1AR-$Y271F^{7.36}$) to remove the nucleophilic reactivity of the

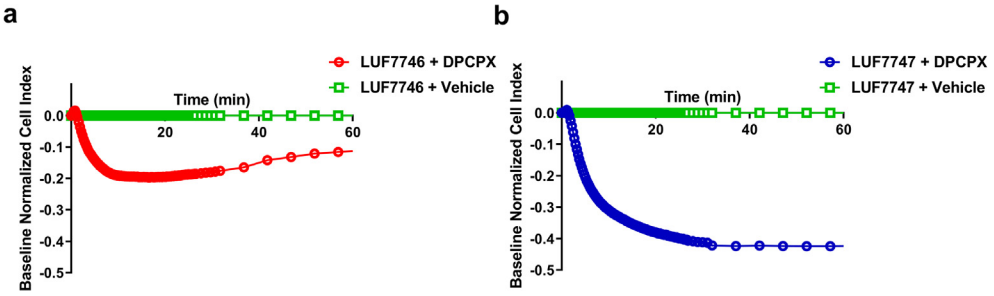

Fig. 8. Characterization of the irreversible receptor activation induced by LUF7746 in a label-free whole cell assay. CHO-hA_1AR-low cells were pre-incubated with 1 μM LUF7746 (a) or LUF7747 (b) for 30 min, followed by the addition of vehicle (0.25% DMSO) or 100 nM DPCPX (in 0.25% DMSO) to track the cell index changes for another 60 min. Representative graphs from one experiment performed in duplicate.

phenolic hydroxyl group and potentially prevent the covalent bond from being formed. Since control compound LUF7747 showed a similar affinity for both the Y271F$^{7.36}$ and WT receptors (Table 1), we assumed that the difference in radioligand binding recovery was not due to a point mutation within the receptor binding site, which has the potential to affect ligand binding properties. Moreover, there were no marked affinity differences on hA$_1$AR-Y271F$^{7.36}$ between LUF7746 (pIC$_{50}$ = 7.2 ± 0.05) and LUF7747 (pIC$_{50}$ = 7.0 ± 0.06). This suggests that the chemically dissimilar ligands LUF7746 (reactive) and LUF7747 (nonreactive) exhibit a similar binding interaction with hA$_1$AR-Y271F$^{7.36}$. Lastly, the extensive washing treatment caused a four-fold increase of [^{3}H]DPCPX binding recovery on hA$_1$AR-Y271F$^{7.36}$ pre-incubated with LUF7746 (Fig. 4b), which is in sharp contrast to the findings in the wild type washout assay. Hence, we concluded Y271$^{7.36}$ is involved in the covalent attachment of LUF7746's fluorosulfonyl group within the hA$_1$AR binding pocket.

A similar result was observed in the functional [^{35}S]GTPγS binding assay. Since LUF7747 showed a comparable potency for hA$_1$AR-Y271F$^{7.36}$ and hA$_1$AR-WT, the receptor functionality was not altered by the point mutation. Furthermore, receptor stimulation by LUF7746 was largely reversed by DPCPX due to the amino acid Y271$^{7.36}$ mutation, unlike in the WT receptor (Fig. 5c). This marked contrast confirms the hypothesized covalent interaction between ligand and receptor and validates the primary role of the tyrosine residue in the formation of the covalent activation. It may be though, that a second site of covalent interaction exists, as the reversal of the functional effect was not complete under the experimental conditions examined. Similar results from functionalized covalent probes were also obtained on other GPCR subtypes. On M$_1$ and M$_2$ muscarinic receptors, nitrogen mustard analogues alkylate more than one residue besides a well-known reactive centre Asp3.32 [41]. Likewise, on the human cannabinoid CB$_2$ receptor, two possible cysteines were validated to mediate the covalent binding of affinity probe AM1336 [42]. Mutagenesis of nucleophilic residues near the orthosteric binding pocket is useful to study the mode and site of interaction, but may also drive the covalent ligand to react with secondary nucleophilic amino acid residues.

Building on our understanding of the chemical properties of LUF7746, we further performed an *in vitro* A$_1$ receptor-mediated whole-cell assay. To reveal the partial agonistic behaviour, the cell line used for this label-free assay has a relatively low hA$_1$AR expression level (B$_{max}$ = 0.968 ± 0.014 pmol/mg protein for [^{3}H]DPCPX derived from saturation experiments) [25]. In particular, the inhibition of reversible activation (LUF7747, Fig. 8b) demonstrated a continued decrease in cell impedance, whereas covalent activation by LUF7746 (Fig. 8a) was first inhibited by DPCPX, although less than for LUF7747, and appeared to return towards the activation state. Hence, we substantiated that the intrinsic cellular effect induced by LUF7746 is vastly different from cellular responses generated by LUF7747. This phenomenon was found in other studies as well. For instance, in the case of the cannabinoid CB$_1$ receptor, covalent agonist AM841 generates an inhibition on synaptic transmission, which cannot be reversed by antagonist [43]. In another study, Jorg *et al.* found that hA$_1$AR modulation by covalent agonists appeared to be insensitive to post-reversal by antagonist [4].

In conclusion, we report the rational design of non-ribose hA$_1$AR ligand LUF7746, with a chemically reactive electrophilic (SO$_2$F) warhead at a judiciously selected position. A series of assays, comprising time-dependent affinity determination, kinetic assay, washout experiments and [^{35}S]GTPγS binding assays, then validated LUF7746 as the first covalent partial agonist for the hA$_1$AR. A combined *in silico* hA$_1$AR-structure based docking and site-directed mutagenesis-study was performed to demonstrate amino acid residue Y271$^{7.36}$ was responsible for the covalent interaction. Furthermore, we demonstrated that LUF7746 behaved as covalent partial agonist under near-physiological conditions at the cellular level. Thus, our covalent ligand LUF7746 behaves as a covalent partial agonist on membranes and intact cells and may serve as a tool compound for further studies on receptor desensitization or internalization and target validation in *in vivo* studies. This useful approach for investigating ligand-receptor interactions can be enhanced through the design of other higher affinity electrophiles, and it can be applied to study molecular mechanisms involved in partial agonism. Future work in this regard would serve to map structural features and the topology of the hA$_1$AR non-ribose partial agonist binding pocket.

CRediT authorship contribution statement

Xue Yang: Conceptualization, Investigation, Writing - original draft, Writing - review & editing. **Majlen A. Dilweg:** Investigation, Writing - original draft, Writing - review & editing. **Dion Osemwengie:** Investigation. **Lindsey Burggraaff:** Investigation. **Daan van der Es:** Conceptualization, Writing - original draft, Writing - review & editing. **Laura H. Heitman:** Conceptualization, Writing - original draft, Writing - review & editing. **Adriaan P. IJzerman:** Conceptualization, Writing - original draft, Writing - review & editing.

Declaration of Competing Interest

The authors declare that they have no known competing financial interests or personal relationships that could have appeared to influence the work reported in this paper.

Acknowledgement

Xue Yang was financially supported by a grant from the Chinese Scholarship Council.

References

[1] A.S. Hauser, M.M. Attwood, M. Rask-Andersen, H.B. Schiöth, D.E. Gloriam, Trends in GPCR drug discovery: new agents, targets and indications, Nat Rev Drug Discov. 16 (12) (2017) 829–842, https://doi.org/10.1038/nrd.2017.178.
[2] D. Weichert, P. Gmeiner, Covalent molecular probes for class A G protein-coupled receptors: advances and applications, ACS Chem. Biol. 10 (6) (2015) 1376–1386, https://doi.org/10.1021/acschembio.5b00070.
[3] D.W. Szymanski, M. Papanastasiou, K. Melchior, N. Zvonok, R.W. Mercier, D.R. Janero, et al., Mass spectrometry-based proteomics of human cannabinoid receptor 2: covalent cysteine 6.47(257)-ligand interaction affording megagonist receptor activation, J. Proteome Res. 10 (10) (2011) 4789–4798, https://doi.org/10.1021/pr2005583.
[4] M. Jörg, A. Glukhova, A. Abdul-Ridha, E.A. Vecchio, A.T.N. Nguyen, P.M. Sexton, et al., Novel irreversible agonists acting at the A$_1$ adenosine receptor, J. Med. Chem. 59 (24) (2016) 11182–11194, https://doi.org/10.1021/acs.jmedchem.6b01561.
[5] K.A. Jacobson, S. Barone, U. Kammula, G.L. Stiles, Electrophilic derivatives of purines as irreversible inhibitors of A$_1$ adenosine receptors, J. Med. Chem. 32 (5) (1989) 1043–1051, https://doi.org/10.1021/jm00125a019.
[6] J. Zhang, L. Belardinelli, K.A. Jacobson, D.H. Otero, S.P. Baker, Persistent activation by and receptor reserve for an irreversible A$_1$-adenosine receptor agonist in DDT$_1$ MF-2 cells and in guinea pig heart, Mol. Pharmacol. 52 (3) (1997) 491–498, https://doi.org/10.1124/mol.52.3.491.
[7] W.F. Kiesman, E. Elzein, J. Zablocki, A$_1$ adenosine receptor antagonists, agonists, and allosteric enhancers, in: C.N. Wilson, S.J. Mustafa (Eds.), Adenosine Receptors in Health and Disease, Handbook of Experimental Pharmacology, Springer, Berlin, Heidelberg, 2009, pp. 25–58.
[8] S.J. Greene, H.N. Sabbah, J. Butler, A.A. Voors, B.E. Albrecht-Küpper, H.-D. Düngen, et al., Partial adenosine A$_1$ receptor agonism: a potential new therapeutic strategy for heart failure, Heart Fail. Rev. 21 (1) (2016) 95–102, https://doi.org/10.1007/s10741-015-9522-7.
[9] L.C.W. Chang, J.K. von Frijtag Drabbe Künzel, T. Mulder-Krieger, R.F. Spanjersberg, S.F. Roerink, G. van den Hout, et al., A series of ligands displaying a remarkable agonistic-antagonistic profile at the adenosine A$_1$ receptor, J. Med. Chem. 48 (6) (2005) 2045–2053, https://doi.org/10.1021/jm049597+.
[10] W. Sherman, T. Day, M.P. Jacobson, R.A. Friesner, R. Farid, Novel procedure for modeling ligand/receptor induced fit effects, J. Med. Chem. 49 (2) (2006) 534–553, https://doi.org/10.1021/jm050540c.
[11] U. Rosentreter, R. Henning, M. Bauser, T. Krämer, A. Vaupel, W. Hübsch, et al., Substituted 2-thio-3,5-dicyano-4-aryl-6-aminopyridines and the use thereof as adenosine receptor ligands, WO2001/025210 A2, April 12, 2001.
[12] J. Louvel, D. Guo, M. Agliardi, T.A.M. Mocking, R. Kars, T.P. Pham, et al., Agonists for the adenosine A$_1$ receptor with tunable residence time. A case for nonribose 4-amino-6-aryl-5-cyano-2-thiopyrimidines, J. Med. Chem. 57 (8) (2014) 3213–3222, https://doi.org/10.1021/jm401643m.
[13] L.H. Heitman, A. Göblyös, A.M. Zweemer, R. Bakker, T. Mulder-Krieger, J.P.D. van Veldhoven, et al., A series of 2,4-disubstituted quinolines as a new class of allosteric

enhancers of the adenosine A_3 receptor, J. Med. Chem. 52 (4) (2009) 926–931, https://doi.org/10.1021/jm8014052.
[14] X. Yang, G. Dong, T.J.M. Michiels, E.B. Lenselink, L.H. Heitman, J. Louvel, et al., A covalent antagonist for the human adenosine A_{2A} receptor, Purinergic Signal. 13 (2) (2017) 191–201, https://doi.org/10.1007/s11302-016-9549-9.
[15] O. Boussif, F. Lezoualc'h, M.A. Zanta, M.D. Mergny, D. Scherman, B. Demeneix, et al., A versatile vector for gene and oligonucleotide transfer into cells in culture and in vivo: polyethylenimine, Proc. Natl. Acad. Sci. U.S.A. 92 (16) (1995) 7297–7301, https://doi.org/10.1073/pnas.92.16.7297.
[16] D. Guo, E.J.H. van Dorp, T. Mulder-Krieger, J.P.D. van Veldhoven, J. Brussee, A.P. IJzerman, et al., Dual-point competition association assay: a fast and high-throughput kinetic screening method for assessing ligand-receptor binding kinetics, J. Biomol. Screening 18 (3) (2013) 309–320, https://doi.org/10.1177/1087057112464776.
[17] L. Xia, A. Kyrizaki, D.K. Tosh, T.T. van Duijl, J.C. Roorda, K.A. Jacobson, et al., A binding kinetics study of human adenosine A_3 receptor agonists, Biochem. Pharmacol. (Amsterdam, Neth) 153 (2018) 248–259, https://doi.org/10.1016/j.bcp.2017.12.026.
[18] Schrödinger Release 2018-3: LigPrep, S, LLC, New York, NY, 2018.
[19] A. Glukhova, D.M. Thal, A.T. Nguyen, E.A. Vecchio, M. Jörg, P.J. Scammells, et al., Structure of the adenosine A_1 receptor reveals the basis for subtype selectivity, Cell 168 (5) (2017) 867–877, https://doi.org/10.1016/j.cell.2017.01.042.
[20] H.M. Berman, J. Westbrook, Z. Feng, G. Gilliland, T.N. Bhat, H. Weissig, et al., The protein data bank, Nucl. Acids Res. 28 (1) (2000) 235–242, https://doi.org/10.1093/nar/28.1.235.
[21] Schrödinger Release 2017-4: Prime, S, LLC, New York, NY, 2017.
[22] D. Guo, T. Mulder-Krieger, A.P. IJzerman, L.H. Heitman, Functional efficacy of adenosine A_{2A} receptor agonists is positively correlated to their receptor residence time, Brit J. Pharmacol. 166 (6) (2012) 1846–1859, https://doi.org/10.1111/j.1476-5381.2012.01897.x.
[23] J.M. Hillger, J. Schoop, D.I. Boomsma, P.E. Slagboom, A.P. IJzerman, L.H. Heitman, Whole-cell biosensor for label-free detection of GPCR-mediated drug responses in personal cell lines, Biosens. Bioelectron. 74 (2015) 233–242, https://doi.org/10.1016/j.bios.2015.06.031.
[24] N. Yu, J.M. Atienza, J. Bernard, S. Blanc, J. Zhu, X. Wang, et al., Real-time monitoring of morphological changes in living cells by electronic cell sensor arrays: an approach to study G protein-coupled receptors, Anal. Chem. (Washington, DC, U S). 78 (1) (2006) 35–43, https://doi.org/10.1021/ac051695v.
[25] A. Dalpiaz, A. Townsend-Nicholson, M.W. Beukers, P.R. Schofield, A.P. IJzerman, Thermodynamics of full agonist, partial agonist, and antagonist binding to wild-type and mutant adenosine A_1 receptors, Biochem. Pharmacol. (Amsterdam, Neth.) 56 (11) (1998) 1437–1445, https://doi.org/10.1016/s0006-2952(98)00202-0.
[26] Y. Cheng, W.H. Prusoff, Relationship between inhibition constant (K_I) and concentration of inhibitor which causes 50 per cent inhibition (I_{50}) of an enzymatic-reaction, Biochem. Pharmacol. (Amsterdam, Neth.) 22 (23) (1973) 3099–3108, https://doi.org/10.1016/0006-2952(73)90196-2.
[27] H.J. Motulsky, L.C. Mahan, The kinetics of competitive radioligand binding predicted by the law of mass action, Mol. Pharmacol. 25 (1) (1984) 1–9.
[28] J. Louvel, D. Guo, M. Soethoudt, T.A.M. Mocking, E.B. Lenselink, T. Mulder-Krieger, et al., Structure-kinetics relationships of Capadenoson derivatives as adenosine A_1 receptor agonists, Eur. J. Med. Chem. 101 (2015) 681–691, https://doi.org/10.1016/j.ejmech.2015.07.023.
[29] D. Guo, S.N. Venhorst, A. Massink, J.P.D. van Veldhoven, G. Vauquelin, A.P. IJzerman, et al., Molecular mechanism of allosteric modulation at GPCRs: insight from a binding kinetics study at the human A_1 adenosine receptor, Brit. J. Pharmacol. 171 (23) (2014) 5295–5312, https://doi.org/10.1111/bph.12836.
[30] P.G. Strange, Use of the GTPγS ([^{35}S]GTPγS and Eu-GTPγS) binding assay for analysis of ligand potency and efficacy at G protein-coupled receptors, Brit. J. Pharmacol. 161 (6) (2010) 1238–1249, https://doi.org/10.1111/j.1476-5381.2010.00963.x.
[31] A. Townsend-Nicholson, P.R. Schofield, A threonine residue in the seventh transmembrane domain of the human A_1 adenosine receptor mediates specific agonist binding, J. Biol. Chem. 269 (4) (1994) 2373–2376.
[32] T. Hua, K. Vemuri, S.P. Nikas, R.B. Laprairie, Y. Wu, L. Qu, et al., Crystal structures of agonist-bound human cannabinoid receptor CB_1, Nature 547 (7664) (2017) 468–471, https://doi.org/10.1038/nature23272.
[33] H. Suga, F.J. Ehlert, Effects of asparagine mutagenesis of conserved aspartic acids in Helix 2 (D2.50) and 3 (D3.32) of M_1–M_4 muscarinic receptors on the irreversible binding of nitrogen mustard analogs of acetylcholine and McN-A-343, Biochemistry 52 (29) (2013) 4914–4928, https://doi.org/10.1021/bi4003698.
[34] C. Li, W. Xu, S.K. Vadivel, P. Fan, A. Makriyannis, High affinity electrophilic and photoactivatable covalent endocannabinoid probes for the CB_1 receptor, J. Med. Chem. 48 (20) (2005) 6423–6429, https://doi.org/10.1021/jm050272i.
[35] L. Xia, H. de Vries, A.P. IJzerman, L.H. Heitman, Scintillation proximity assay (SPA) as a new approach to determine a ligand's kinetic profile. A case in point for the adenosine A_1 receptor, Purinergic Signall. 12 (1) (2016) 115–126, https://doi.org/10.1007/s11302-015-9485-0.
[36] M.L.J. Doornbos, X. Wang, S.C. Vermond, L. Peeters, L. Pérez-Benito, A.A. Trabanco, et al., Covalent allosteric probe for the metabotropic glutamate receptor 2: design, synthesis, and pharmacological characterization, J. Med. Chem. 62 (1) (2019) 223–233, https://doi.org/10.1021/acs.jmedchem.8b00051.
[37] K.W. Figueroa, H. Suga, F.J. Ehlert, Investigating the interaction of McN-A-343 with the M_1 muscarinic receptor using its nitrogen mustard derivative and ACh mustard, Brit. J. Pharmacol. 160 (6) (2010) 1534–1549, https://doi.org/10.1111/j.1476-5381.2010.00810.x.
[38] D. Weichert, A.C. Kruse, A. Manglik, C. Hiller, C. Zhang, H. Hübner, et al., Covalent agonists for studying G protein-coupled receptor activation, Proc. Natl. Acad. Sci. U.S.A. 111 (29) (2014) 10744–10748, https://doi.org/10.1073/pnas.1410415111.
[39] C.J. Draper-Joyce, M. Khoshouei, D.M. Thal, Y.L. Liang, A.T.N. Nguyen, S.G.B. Furness, et al., Structure of the adenosine-bound human adenosine A_1 receptor-G_i complex, Nature 558 (7711) (2018) 559–563, https://doi.org/10.1038/s41586-018-0236-6.
[40] L.H. Heitman, T. Mulder-Krieger, R.F. Spanjersberg, J.K. von Frijtag Drabbe Künzel, A. Dalpiaz, A.P. IJzerman, Allosteric modulation, thermodynamics and binding to wild-type and mutant (T277A) adenosine A_1 receptors of LUF5831, a novel non-adenosine-like agonist, Brit. J. Pharmacol. 147 (5) (2006) 533–541, https://doi.org/10.1038/sj.bjp.0706655.
[41] H. Suga, G.W. Sawyer, F.J. Ehlert, Mutagenesis of nucleophilic residues near the orthosteric binding pocket of M_1 and M_2 muscarinic receptors: effect on the binding of nitrogen mustard analogs of acetylcholine and McN-A-343, Mol. Pharmacol. 78 (4) (2010) 745–755, https://doi.org/10.1124/mol.110.065367.
[42] R.W. Mercier, Y. Pei, L. Pandarinathan, D.R. Janero, J. Zhang, A. Makriyannis, hCB2 ligand-interaction landscape: cysteine residues critical to biarylpyrazole antagonist binding motif and receptor modulation, Chem. Biol. 17 (10) (2010) 1132–1142, https://doi.org/10.1016/j.chembiol.2010.08.010.
[43] C.M. Keenan, M.A. Storr, G.A. Thakur, J.T. Wood, J. Wager-Miller, A. Straiker, et al., AM841, a covalent cannabinoid ligand, powerfully slows gastrointestinal motility in normal and stressed mice in a peripherally restricted manner, Brit. J. Pharmacol. 172 (9) (2015) 2406–2418, https://doi.org/10.1111/bph.13069.